2017-12

# Finite element analysis of particle ionization within carbon nanotube ion micro thruster

Fiebrandt, Jamison R.

Monterey, California: Naval Postgraduate School


# NAVAL POSTGRADUATE SCHOOL

**MONTEREY, CALIFORNIA**

# THESIS

**FINITE ELEMENT ANALYSIS OF PARTICLE IONIZATION WITHIN CARBON NANOTUBE ION MICRO THRUSTER**

by

Jamison R. Fiebrandt

December 2017

Thesis Advisor: Dragoslav Grbovic
Co-Advisor: Emil Kartalov

THIS PAGE INTENTIONALLY LEFT BLANK

| REPORT DOCUMENTATION PAGE | | | *Form Approved OMB No. 0704–0188* |
|---|---|---|---|



| **1. AGENCY USE ONLY** | **2. REPORT DATE** December 2017 | **3. REPORT TYPE AND DATES COVERED** Master's thesis |
|---|---|---|

| **4. TITLE AND SUBTITLE** FINITE ELEMENT ANALYSIS OF PARTICLE IONIZATION WITHIN CARBON NANOTUBE ION MICRO THRUSTER | **5. FUNDING NUMBERS** |
|---|---|
| **6. AUTHOR(S)** Jamison R. Fiebrandt | |
| **7. PERFORMING ORGANIZATION NAME(S) AND ADDRESS(ES)** Naval Postgraduate School Monterey, CA 93943-5000 | **8. PERFORMING ORGANIZATION REPORT NUMBER** |
| **9. SPONSORING /MONITORING AGENCY NAME(S) AND ADDRESS(ES)** N/A | **10. SPONSORING / MONITORING AGENCY REPORT NUMBER** |

**11. SUPPLEMENTARY NOTES** The views expressed in this thesis are those of the author and do not reflect the official policy or position of the Department of Defense or the U.S. Government. IRB number ____N/A____.

| **12a. DISTRIBUTION / AVAILABILITY STATEMENT** Approved for public release. Distribution is unlimited. | **12b. DISTRIBUTION CODE** A |
|---|---|

**13. ABSTRACT (maximum 200 words)**

As electric propulsion becomes more of a viable option for satellite station keeping, MEMS electrodes are being more thoroughly investigated for their operational capacity. Computer modelling simulations of the particle physics involved during the initial ionization events of plasma generation have proven reliable in determining the effectiveness of carbon nanotube-covered nozzles. Two different simulations, comparing angled-wall etched nozzles with and without CNT deposition, demonstrated improvement of ion beam current when the walls are lined with carbon nanotubes. These models agree well with experimental results in the initial ionization event regime. Further investigation of complete plasma physics simulation and ionization parameter characterization are required to refine the simulation before it is a complete, viable system for thruster design optimization.

| **14. SUBJECT TERMS** space propulsion, miniature ion thruster, ionization simulation, carbon nanotube simulation, microsatellite, finite element analysis, electric field, particle tracing | **15. NUMBER OF PAGES** 55 |
|---|---|
| | **16. PRICE CODE** |

| **17. SECURITY CLASSIFICATION OF REPORT** | **18. SECURITY CLASSIFICATION OF THIS PAGE** | **19. SECURITY CLASSIFICATION OF ABSTRACT** | **20. LIMITATION OF ABSTRACT** |
|---|---|---|---|
| Unclassified | Unclassified | Unclassified | UU |

NSN 7540–01-280-5500 Standard Form 298 (Rev. 2–89) Prescribed by ANSI Std. 239–18

THIS PAGE INTENTIONALLY LEFT BLANK

**Approved for public release. Distribution is unlimited.**

# FINITE ELEMENT ANALYSIS OF PARTICLE IONIZATION WITHIN CARBON NANOTUBE ION MICRO THRUSTER

Jamison R. Fiebrandt
Lieutenant, United States Navy
B.S., University of South Florida, 2011

Submitted in partial fulfillment of the
requirements for the degree of

**MASTER OF SCIENCE IN APPLIED PHYSICS**

from the

**NAVAL POSTGRADUATE SCHOOL**
**December 2017**

Approved by: Dragoslav Grbovic, Ph.D.
Thesis Advisor

Emil Kartalov, Ph.D.
Co-Advisor

Kevin Smith, Ph.D.
Chair, Department of Physics

THIS PAGE INTENTIONALLY LEFT BLANK

# ABSTRACT

As electric propulsion becomes more of a viable option for satellite station keeping, MEMS electrodes are being more thoroughly investigated for their operational capacity. Computer modelling simulations of the particle physics involved during the initial ionization events of plasma generation have proven reliable in determining the effectiveness of carbon nanotube-covered nozzles. Two different simulations, comparing angled-wall etched nozzles with and without CNT deposition, demonstrated improvement of ion beam current when the walls are lined with carbon nanotubes. These models agree well with experimental results in the initial ionization event regime. Further investigation of complete plasma physics simulation and ionization parameter characterization are required to refine the simulation before it is a complete, viable system for thruster design optimization.

THIS PAGE INTENTIONALLY LEFT BLANK

# TABLE OF CONTENTS

THIS PAGE INTENTIONALLY LEFT BLANK

# LIST OF FIGURES

# LIST OF TABLES

THIS PAGE INTENTIONALLY LEFT BLANK

# LIST OF ACRONYMS AND ABBREVIATIONS

| | |
|---|---|
| EP | electric propulsion |
| CRT | cathode ray tube |
| CNT | carbon nanotube |
| SEM | scanning electron microscope |
| IA | ionization area |

THIS PAGE INTENTIONALLY LEFT BLANK

# ACKNOWLEDGMENTS

First and foremost, I would like to thank the NPS Physics department for the tremendous opportunity to fulfil a childhood dream of spacecraft design. Without the tools and facilities provided, I would never have been able to have started. My appreciation to Dr. Grbovic for his unending enthusiasm for the project and constant guidance in scope of the research, which kept me focused and on subject to produce a product worthy of industry.

My deepest thanks to Dr. Emil Kartalov for his project approach guidance and writing strategy. I also greatly value his instinctual simple approach to a complex problem when things became too much to consider.

Finally, I would like to thank my project partner, LT Bryan Crosby, for being a part of the process, each step of the way. His experimental system steered many of the ideas in this research, and his approach helped to determine its effectiveness.

THIS PAGE INTENTIONALLY LEFT BLANK

# I. INTRODUCTION

A common problem in space flight propulsion is fuel capacity for mission longevity, and dangers to personnel and mission due to the use of volatile chemical fuels. Electric propulsion greatly reduces these risks and is a highly desirable replacement to traditional propulsion. An added benefit is the potential of electronic propulsion technology to be miniaturized and applied to nanosatellites, known as CubeSats.

CubeSats are small satellites on the size in units of U long, 1U=10cm x 10cm x 10cm. These are usually deployed via spring-loaded launcher from a rocket vehicle that is carrying a much larger, more valuable payload [1]. Sometimes the CubeSat launcher has a very close proximity to the primary burner on the vehicle (Figure 1). Due to CubeSats' tagalong nature, launch vehicle developers usually do not allow compressed gas or flammable fuels, which cause a higher and unacceptable risk to the launch of the primary mission, to be used for CubeSat propulsion.

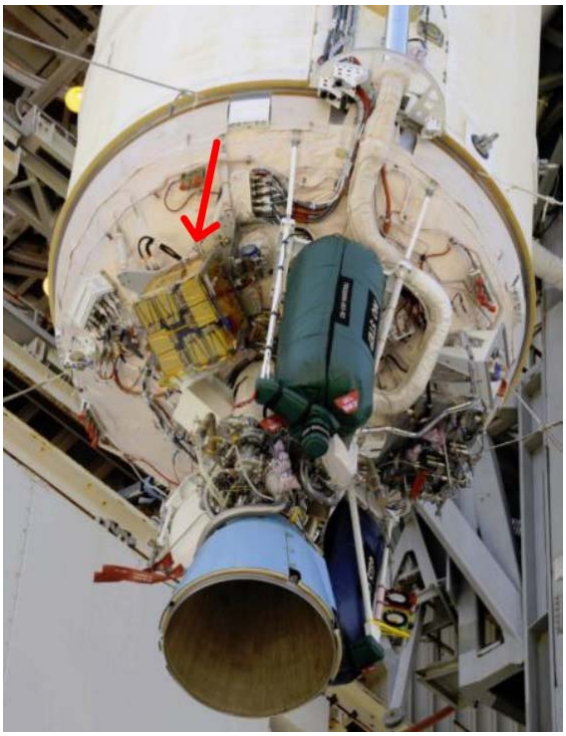

Figure 1. OUTSat mated to NROL-36 mission. Adapted from [1].

Electric propulsion (EP) is an alternative to the dangerous fuels that are an issue for CubeSat vehicle launchers, while providing additional benefits such as longer time of use and fuel efficiency. EP uses an electrical force to accelerate a charged particle, also known as an ion, away from the spacecraft [2]. Newton's third law of motion applies, and as both the particle and space craft move away from each other, the space craft experiences a thrust. The concept of EP was originally discussed with the invention of the cathode ray tube (CRT) [3]. There exist three distinct types of particle accelerator thrusters: electro thermal, electrostatic, and electromagnetic. This thesis investigates the use of an electrostatic thruster, miniaturized for a nanosatellite.

# II. THE PHYSICS

The ion thruster is a form of electric propulsion where charged particles are accelerated away from an object to impart a thrust on the object. The thrust is governed by the Newton's third law of motion, commonly referred to as "for every action, there is an equal and opposite reaction," or momentum is conserved in a system of two or more interacting masses.

$$m_1 v_1 = m_2 v_2 \tag{2.1}$$

where $m_1$, $m_2$ are the masses and $v_1$, $v_2$ are the velocities of the two objects.

Ions are electrically charged atoms, either negatively with excess of electrons, or positively with deficiency of electrons, compared to the charge of the nucleus. When charged particles are subjected to electric or magnetic field, they are forced away from the thruster. Consequently, to conserve momentum, the charged particle pushes back onto the source of this field and thus a thrust is generated. In an electrostatic thruster, ion plasma is subjected to an electric field and accelerated away, exerting a force on the system attached to the thruster, known as thrust.

## A. IONIZATION

This thesis develops a finite element model for investigating the effects of CNTs on the efficiency of field ionization. In field ionization, an electron is removed from an atom via quantum mechanical tunneling in very high electric fields (usually between 107 to 108 V/cm). The coulombic barrier for the electron is distorted by the applied electric field, facilitating a finite probability of the electron to tunnel through the potential barrier and be absorbed by the source of the electric field [4]. Figure 2 compares the coulombic barrier for the valence electron in an atom and the same subjected to a high electric field.

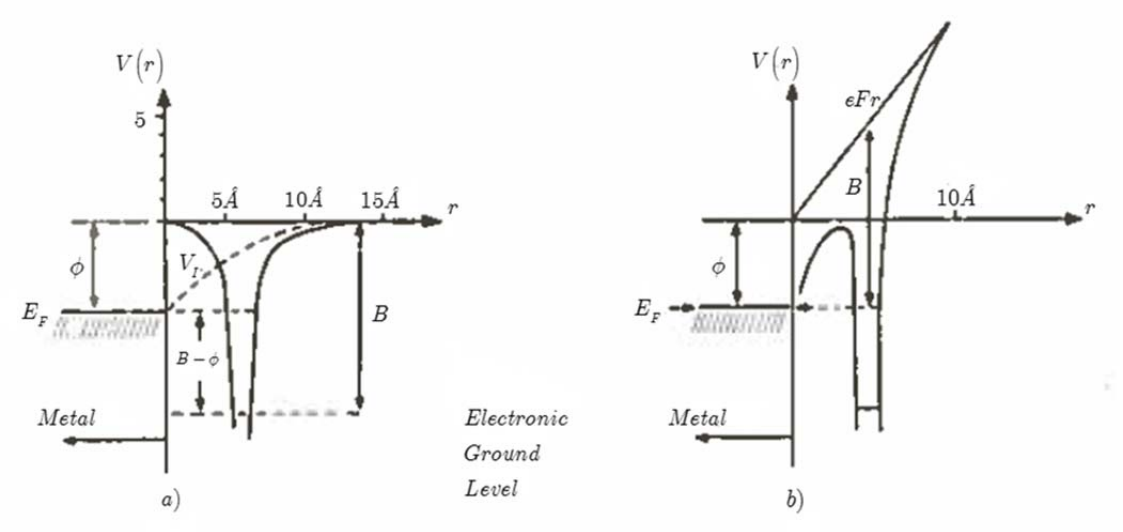


Figure 2. Atom potential well modeling the coulombic barrier (a) and manipulated potential well subjected to an electric field (b). Source: [4]

$E_F$ is the electron binding energy of the atom, e$Fr$ is the applied electric voltage and $V_i$ is the electron image potential. This thesis will model the atomic particles of a gas passing through high electric fields generated at the tips of CNTs. Particles are expected to ionize because electrons have tunneled into the highly conductive CNT via field ionization at very high electric fields being generated at the CNT's tip.

## B. PASCHEN'S LAW

The electric field required to ionize a gas, allowing for electrical current to flow, was empirically defined by Friedrich Paschen in 1889 [5]. Friedrich Paschen characterized the relationship of a gas's breakdown voltage to the pressure of the gas and the separation distance of the electrodes. Breakdown voltage is the voltage required to start a discharge in a gas to create plasma. Paschen developed Equation (2.2),

$$V_B = \frac{Bpd}{ln(Apd) - ln[ln(1 + \frac{1}{\gamma_{se}})]}, \tag{2.2}$$

where $V_B$ is the breakdown voltage, $p$ is the gas pressure, $d$ is the gap distance in meters and $\gamma_{se}$ is the secondary electron emission coefficient. A and B are experimentally

determined constants that vary from gas to gas. When breakdown voltage is plotted versus the pressure of the gas times the electrode separation, a plot known as Paschen's Curve is created. Each gas has slightly different curves due to their own atomic properties. This thesis will later use an experimentally determined Paschen's curve to determine the ionization requirement of argon gas.

## C. THRUSTER CURRENT

After particles are ionized, they are accelerated to the accelerator grid. Charge will arrive at this grid, which also serves as a cathode in this thesis and the experimental setup at NPS, providing an electrical current. Current is defined as the rate of charge:

$$I_{ion} = \frac{dQ}{dt}, \tag{2.3}$$

where $I_{ion}$ is the current in Amperes, $dQ$ is the charge that crosses a plane of the electrode (or reaches the electrode) over a given time $dt$. During ionization, particles ionize and become charged and accelerate in the electric field with a number of them reaching the cathode over a period of time. Current can be determined using the velocity of these charged particles as they travel across the gap between the ionization location and the accelerator grid. Current generated by each individual ion is modelled with Equation (2.4):

$$I_{ion} = \frac{ve}{d}, \tag{2.4}$$

where $v$ is the ion's velocity, $d$ is the distance from the location of the particle's ionization to the accelerator grid and $e$ is the fundamental charge of an electron. The sum of the current of all particles will result in what is called the beam current. This current collected at the accelerator grid of a thruster is used as a measure of the efficiency of an ion thruster as follows [2]:

$$\eta_m = \frac{I_b}{e}\frac{M}{\dot{m}_p}, \tag{2.5}$$

$\eta_m$ is the thruster's mass utilization factor, $I_b$ is the beam current, $e$ is the fundamental charge value, and $M$ and $\dot{m}_p$ are the molar mass and the mass flow rate of the propellant

respectively. The MUF is a measure of the efficiency of ionization and thus the thruster. It states which fraction of all the particles that enter the thruster gets ionized.

## D. FIELD ENHANCEMENT

Field ionization works best at small energy barriers at the surface of the absorbing conductor, permitting a higher probability and thus rate of quantum tunneling [6]. Essentially, strong electric fields very close to an anode are required for ionization to occur. Conveniently, high electric fields are generated at the tips of electrodes [4].

Field emission is the experiment best suited to demonstrate a field enhancement factor as described by R.H. Fowler and L. Nordheim [7]. The Fowler-Nordheim equation is a function of the applied voltage ($V$) and a geometric field enhancement factor ($\beta$):

$$I = \frac{A V^2}{\phi} e^{\left(-\frac{B \phi^{\frac{3}{2}}}{\beta V}\right)}, \tag{2.6}$$

where A and B are constants, $1.541 \times 10^{-6} \ \frac{A \cdot eV}{V^2}$ and $6.831 \times 10^{9} \ \frac{V}{eV^{3/2} \cdot m}$, respectively, and $\phi$ is the work function of the electrode material [8]. It is shown in Equation (2.6) that larger applied voltages, smaller work functions, and larger enhancement factors will result in larger beam current.

Field emission is when an electron emits from an electrode to a gas. However, in this thesis, the electron is tunneling from the gas to the electrode in the reverse process, which is called field ionization. The principles are the same, but the charge value is opposite. Field ionization is thus an extension of the field emission relation. This thesis will model the effects of the small geometric parameters of CNTs at varying voltages on the resulting current.

# III. THE MODEL

There are two major components that need to be defined when designing the model in finite element analysis (FEA) software, COMSOL Multiphysics. These components are the geometry and the mesh. Geometry is the physical shape and size of the design to be modeled and the mesh is segmenting these shapes into smaller pieces so that equations governing the physics can be solved in smaller manageable pieces.

## A. GEOMETRY

This thesis uses the geometry of the nozzles fabricated by ENS Alfred Garvey [9] shown in Figures 3 and 4. Although these nozzles are contoured, which is due to the fabrication process used, the eventual intent is for a conical nozzle.

### 1. The Nozzle

The dimensions of each element in the array of nozzles were measured via the scanning electron microscope (SEM) (Figures 3 through 5). Average dimensions, close to their mean, were used in the model.

Table 1. Nozzle measurements

| | Size (um) |
|---|---|
| Height | 235 |
| Inlet diam. | 800 |
| Outlet diam. | 229 |

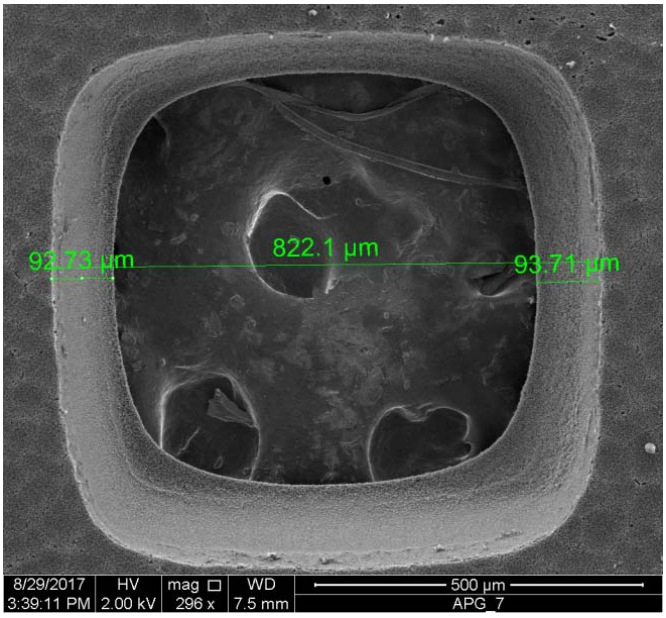


Figure 3. SEM photo of nozzle width

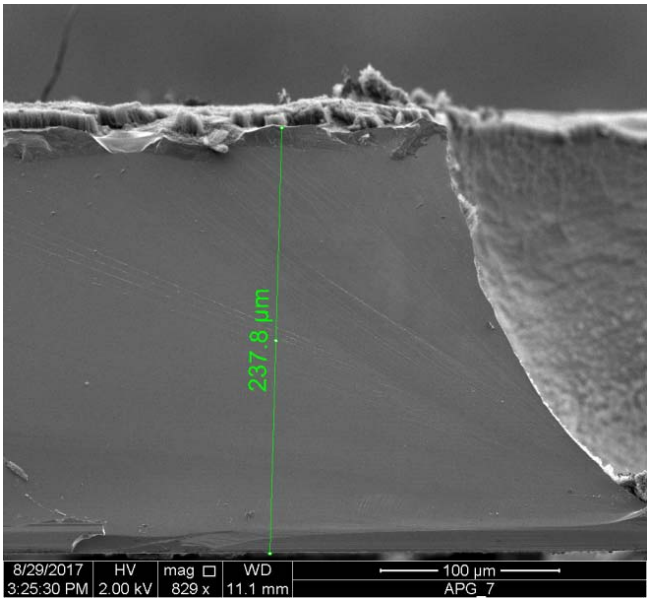


Figure 4. SEM photo of nozzle height

The width of the throat of the nozzle opening was determined using the measured height and then fitting it to a 20-degree nozzle angle. These assumed dimensions made the simulation creation, meshing, and modeling much quicker, facilitating multiple runs repeatedly.

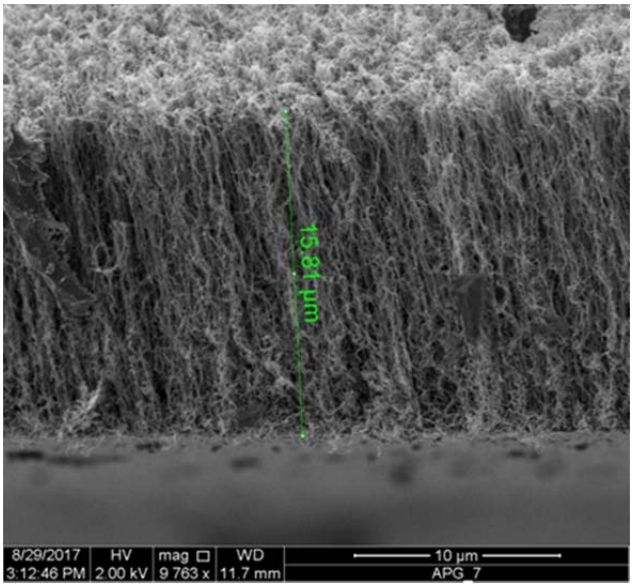


Figure 5. SEM photo of CNT lengths

## 2. Carbon Nanotube Assembly

Of the two models used, one had two metal layers, an aluminum layer and an iron layer, as those were deposited as adhesion layer and catalyst, respectively, in order to obtain vertically grown nanotubes [10]. In the second model, the iron layer was removed and CNTs, evenly spaced along the nozzle inner wall, were added. CNT fabrication consumes the iron layer on which they are deposited; therefore, the model has the CNTs directly joined to the aluminum. Figure 6 compares the two models side by side.

Table 2. Metal layer thicknesses

| | Thickness (um) |
|---|---|
| Aluminum | 0.01 |
| Iron | 0.005 |

Table 3. CNT measurements

| | Size (um) |
|---|---|
| Length | 15 |
| Width | 0.05 |

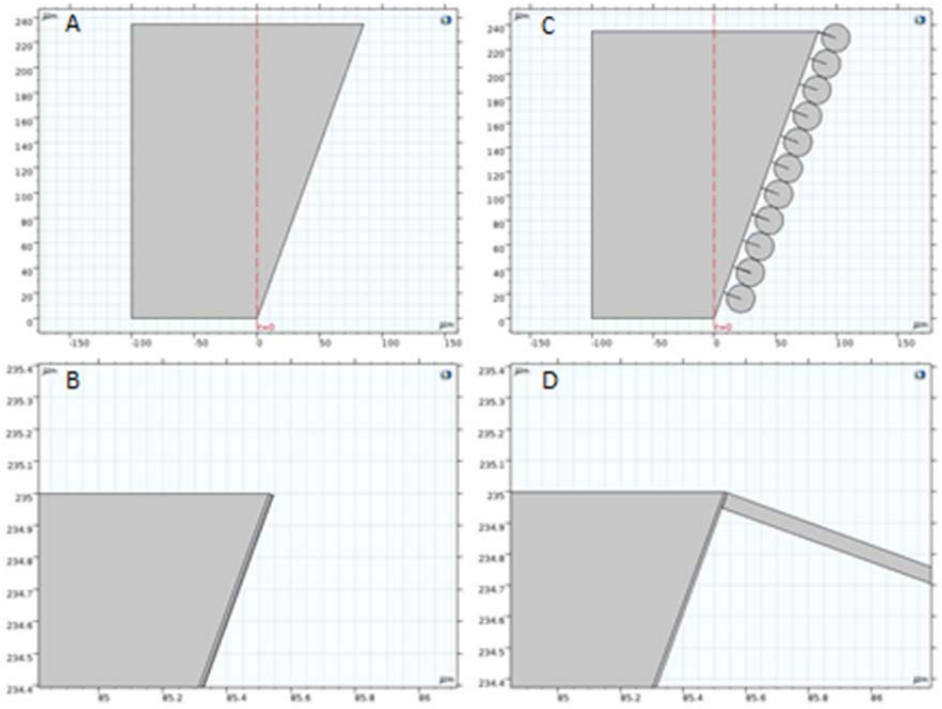


Figure 6. Side-by-side comparison of the two different models

In Figure 6A-Figure 6D, we see a side-by-side comparison of the metalized only model, A and B, versus the CNT grown model C and D. The CNTs were measured in the SEM to be approximately 15 microns long and 5 nm wide. These measurements can be seen in Figure 6C and D, respectively.

Ten CNTs are evenly spaced along the nozzle's wall were used to facilitate a proof of concept of a high localized electric field along equal distances through the depth of the model. A fillet was used on the end of each CNT to match the expected geometry of a CNT's tip.

The CNTs applied to the aluminum layer of the silicon nozzle are shown in Figure 6D. Notice that there is no iron layer in this model, as there is in the metalized-only

model. This is due to the iron being consumed during the CNT growth process. The iron grows upward with the CNTs, existing on the tips and is no longer as a layer.

When meshing, to ensure the electrostatic effects were being modelled properly, additional circles (as seen in Figure 6C) were drawn surrounding CNT tip. This was added in order to be able to have different mesh settings than the remainder of the volume in order to appropriately scale the mesh elements in the local area of the CNT tips.

## B. MESHING

Because the thruster design is on the MEMS (micrometer) scale, our meshing must be appropriately developed to accept the physics and accurately model the physical phenomena in the small spaces. The metal layers, whether it is both aluminum and iron or just aluminum, are the thinnest piece of the design. These regions are meshed first, mapped evenly along the length of the edge at a size that easily fits the width of a CNT. In Figure 7, the sizing is shown and is used on both the blank model and CNT model to maintain consistency.

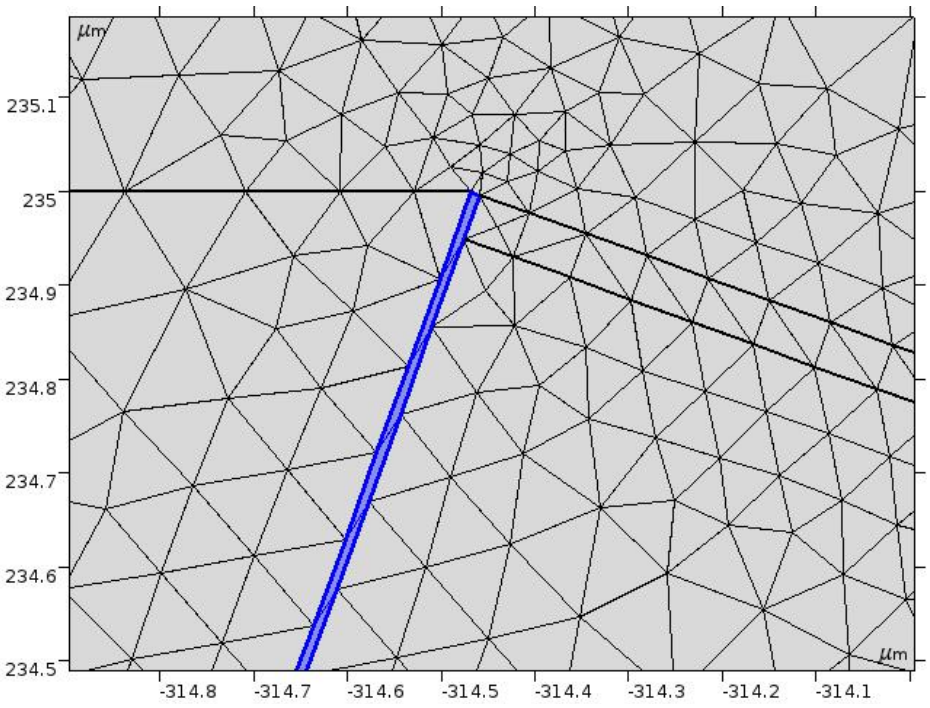


Figure 7. Metal layer mesh rendering

The CNT is meshed from its tip to its base. A boundary layer is defined on the fillet surface of the CNT tip, which is automatically estimated as a triangle in the mesh. Only two boundaries are defined due to negligible effects on the electric field calculated with larger numbers of boundaries. As the mesh is generated along the length of the tube as seen in Figure 8, it creates an evenly spaced element pattern that quickly facilitates an accurate estimate of charge distribution along a uniform conductor.

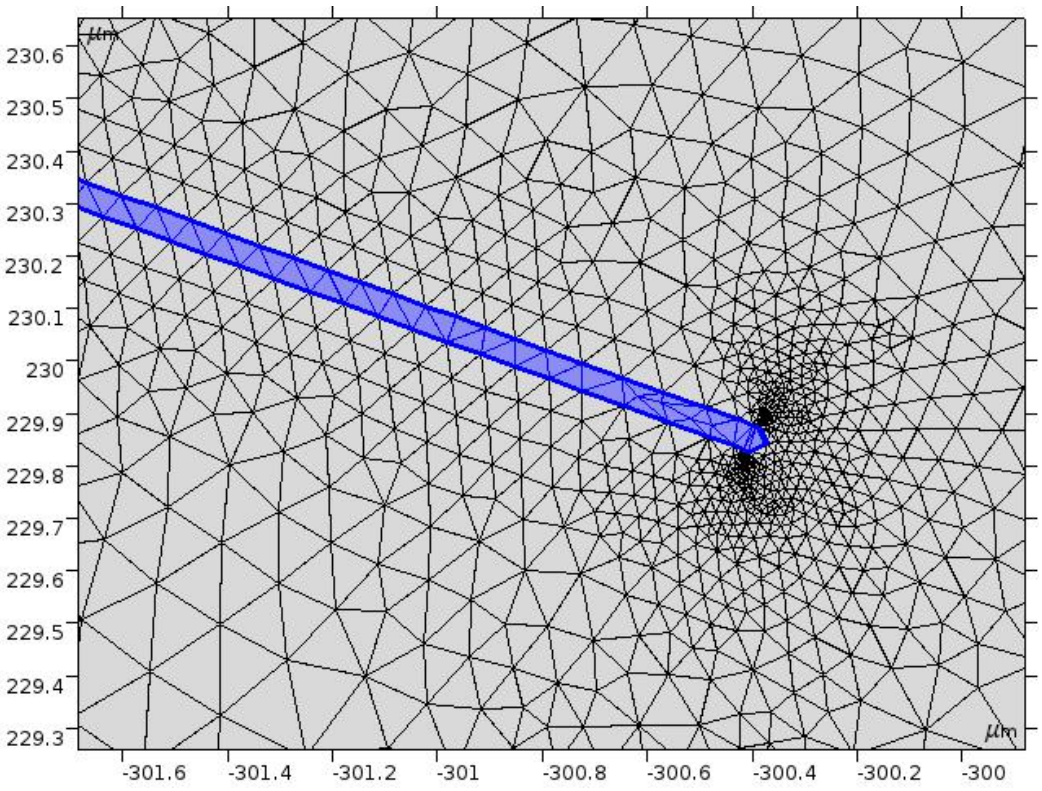


Figure 8. CNT mesh rendering

A high localized electric field is expected to form in the space surrounding the tip of each CNT. A separate circular geometry is drawn in this space so it can be meshed much smaller than the remainder of the volume as shown in Figure 9. The mesh needs to have elements that are equal to or smaller than the electric field enhancement factor. Each circle's size is set to be centered on the tip of each CNT and its edge tangential to the circle adjacent. The mesh is set to Free Triangular on set to an Extra Fine element size.

This decreases the maximum and minimum element sizes to 63.5 and 0.238 um each respectfully. The expectation is to model extremely accurate electric field magnitudes extremely close to the boundary between the CNT and area surrounding.

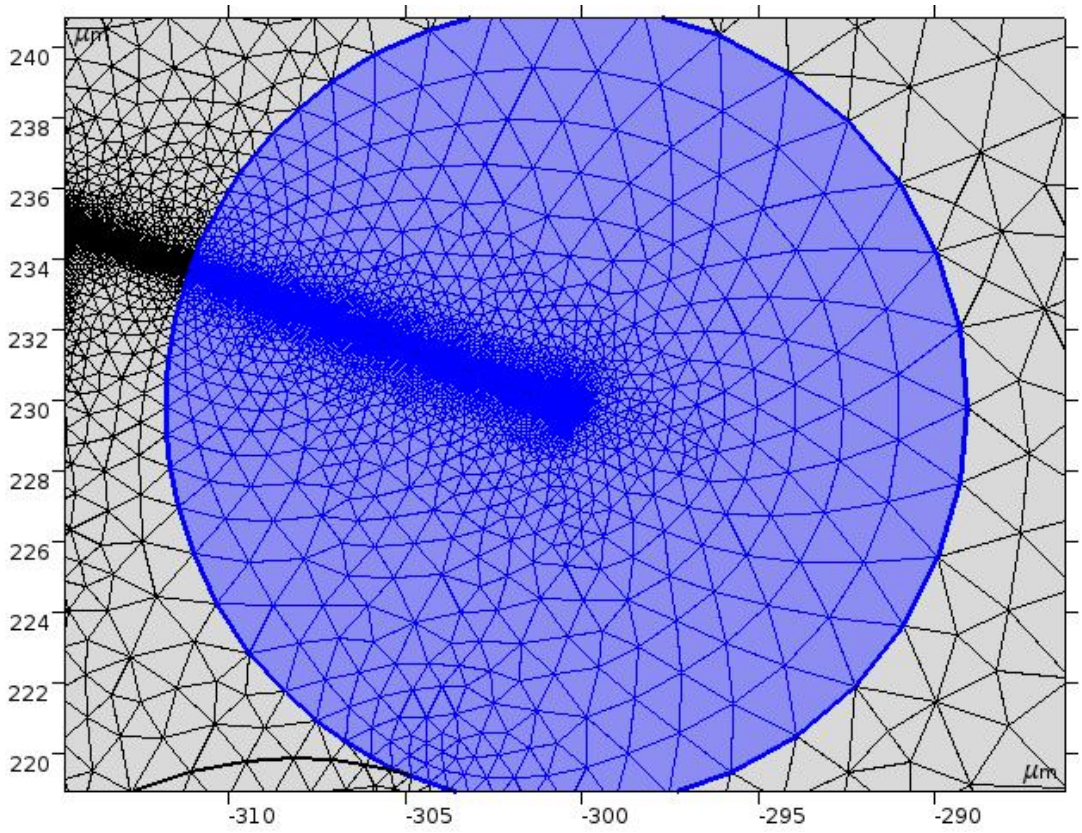


Figure 9. Localized area around the tip of one of the CNTs' mesh rendering

Outside the localized circles, the area is either the inside of the nozzle or the gap between the nozzle and the accelerator grid. Because we are expecting the localization to happen at the tips of the CNT the elements are one size setting larger than the circles, at a maximum and minimum size of 117 or 0.397 um each, in Figure 10.

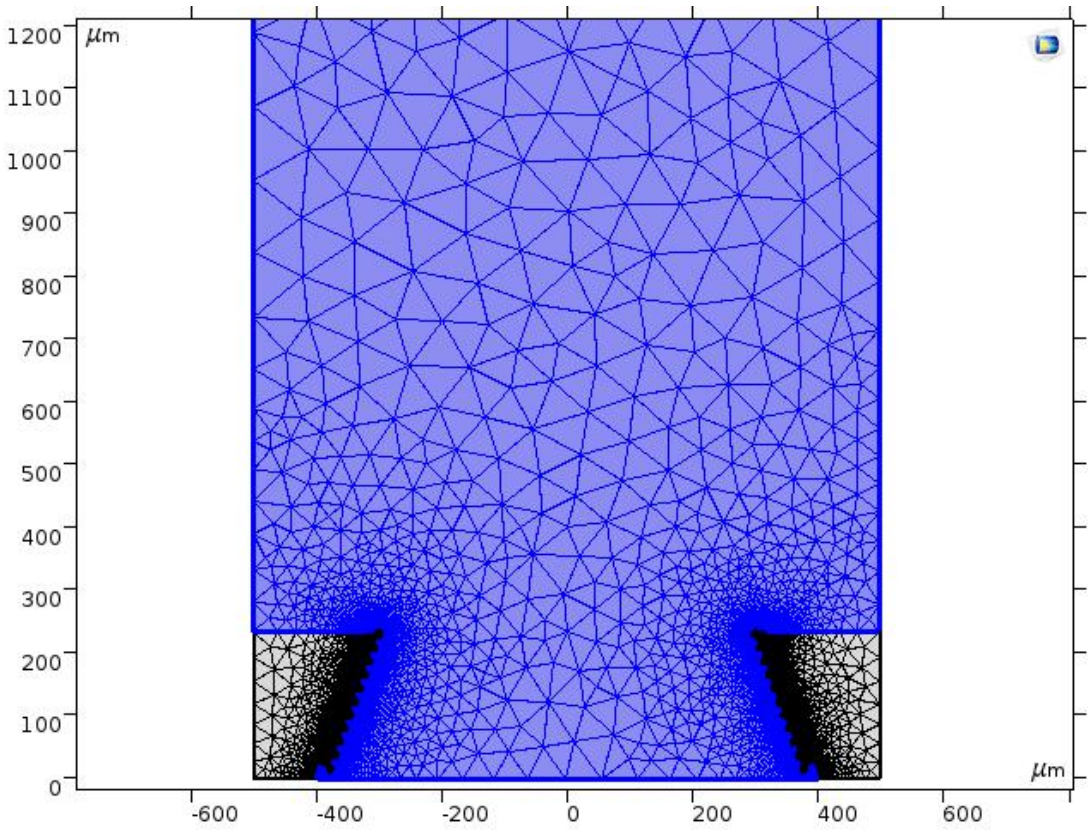


Figure 10. Large volume mesh rendering

These larger elements make evaluating physical quantities in the much larger area significantly quicker without any detriment to the accuracy of the model.

# IV. SIMULATION

The basic design of the micro thruster is an array of nozzles deep reactive ion etched into a $1cm^2$ silicon chip and CNT's grown perpendicular to the surfaces [10]. This nozzle array is charged with a positive potential. Separated some distance from the nozzle array is a finely meshed copper that is used as the accelerator grid. An electrical ground is applied to the grid to create the necessary electric field for ionization and particle acceleration.

## A. ELECTROSTATIC ASSUMPTIONS

Each nozzle is approximately 0.0064 square centimeters and each nozzle array contains 25 nozzles, as seen in Figure 11. This equates to a total area of 0.16 square centimeters, meaning that the total nozzle array makes up 16% of the area of the 1 square centimeter silicon wafer. This entire silicon chip can be estimated to be a single solid plate of carbon nanotubes.

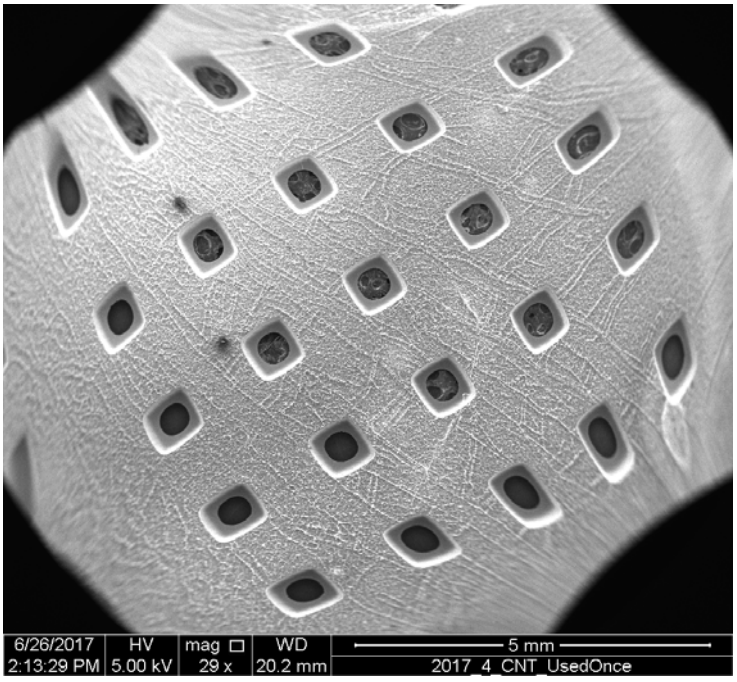


Figure 11. SEM micrograph of full nozzle array

The other half of the system is the accelerator grid's copper mesh. It has an individual opening size of 76 microns resulting in a 35% fill-factor [11]. Each thruster nozzle measures 800 μm across and the array of nozzles is separated by 3600 microns (0.36 cm) from this grid, shown in Figure 12. Because the scale of the mesh versus the total scale of the nozzle including the comparably larger gap distance, it is reasonable to estimate the grid as a sheet metal ground plane.

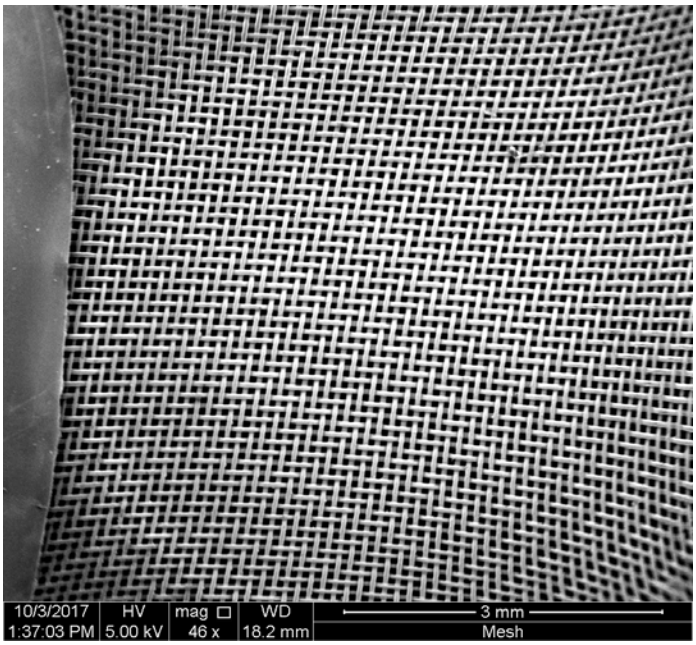


Figure 12. Accelerator grid wire mesh

For the purposes of determining the electro static effects exerted on the argon gas as it flows between the nozzle array and the accelerator grid, it is reasonable to treat the overall assembly as a parallel plate capacitor. This is only to determine the ionization requirement for argon.

## B. PARTICLE ASSUMPTIONS

Each particle entering the nozzle in the simulation is treated as an individual atom of un-ionized Argon; therefore, particles have a mass of $6.633 \times 10^{26}$ kg. Knowing the inlet pressure and the mass flow rate of an experimental setup, the mean free path and initial

velocity of an individual particle can be estimated. This will define initial conditions at the inlet of the particles in the model

$$l = \frac{k_b T}{\sqrt{2}\pi d^2 P} \ , \tag{4.1}$$

where $l$ is the mean free path of a particle, $k_b$ is Boltzman's constant, $d$ is the atomic diameter, $T$ is the temperature of the gas and $P$ is the gas pressure. The mean free path is the average travel length that particles travel between collisions. To set up the conditions so they are as close as possible to the experimental conditions of a concurrent thesis by LT Bryan Crosby, we assume room temperature and an inlet pressure of 40psi and determine the mean free path is 0.4μm [12]. With the diameter of argon at 0.142 nm and an inlet opening 800 μm across, there are approximately 2000 particles spanning the diameter of the nozzle inlet.

The flow of argon into the nozzle is controlled by its mass flow rate $\dot{m}$,

$$\dot{m} = \rho A v \ , \tag{4.2}$$

where $v$ is the particle velocity, $\dot{m}$ is our mass flow rate of the argon, $\rho$ is the density of the argon at room temperature. Rearranging Equation (4.2) results in

$$v = \frac{\dot{m}}{rA} \ . \tag{4.3}$$

Solving Equation 4.3 for the inlet velocity of each electrically neutral particle results 1,523 m/s.

## C. PASCHEN LAW APPLICATION

The Universidad Autonoma Del Estado de Mexico conducted a series of experiments at low pressure and developed the Paschen law for Argon, Figure 13. They tested varying sizes of electrode areas. Each nozzle array in the model is 1 $cm^2$; therefore, we are most interested in their data obtained on a 1-cm diameter electrodes.

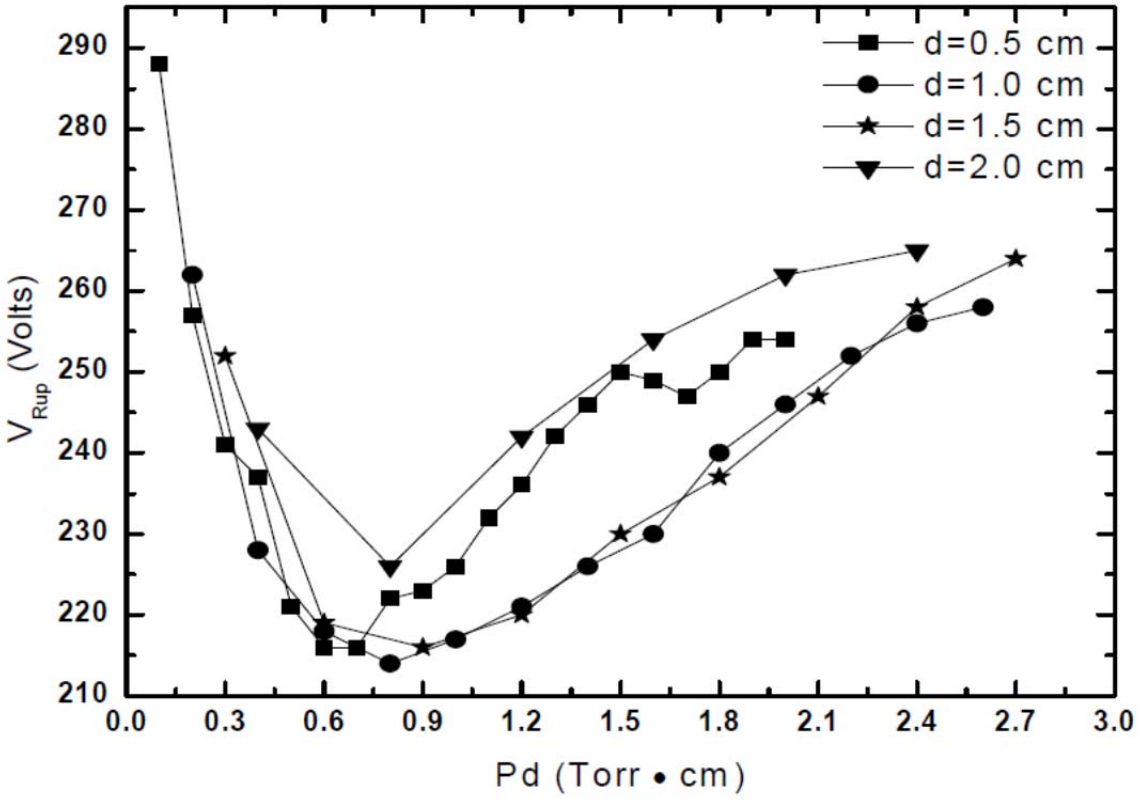


Figure 13. Paschen's curve obtained varying Ar gas pressure and electrode distances. Source: [5].

Torres measured the required voltage for the argon to begin to glow discharge: this is the time when ionization occurs. Using their developed Panchen's curve, it was possible to extrapolate the required voltage for ionization at our pressure and nozzle to acceleration grid gap, Figure 14.

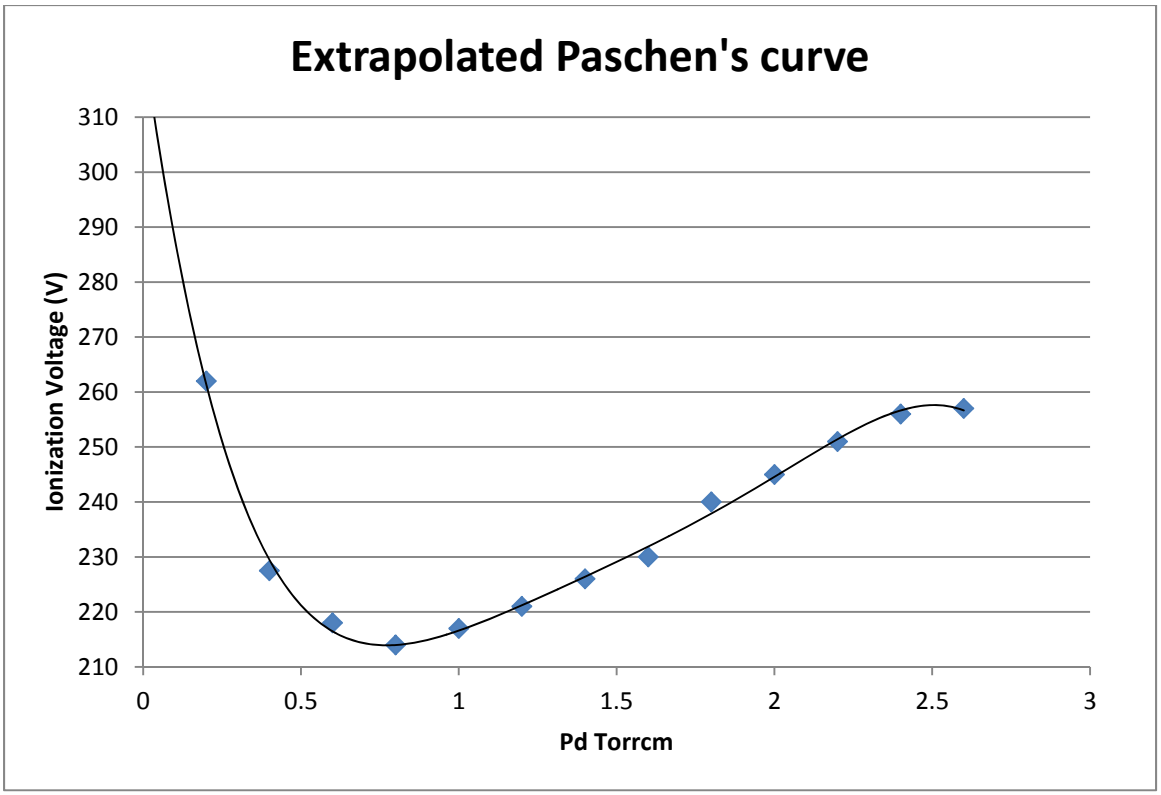


Figure 14. Paschen's curve extrapolated from C. Torres et al. data

This applies, given that the model simulation assumes the assembly as two parallel plates, the same set up used in their apparatus. With a measured gap distance of 0.3175 cm at a vacuum of 51 mTorr, the calculated p*d for this set up is $0.016\,\mathrm{Torr}\cdot\mathrm{cm}$. Averaging the third, fourth and fifth order fitting curves of the experimental data, the required voltage for ionization is found to be 299.96 V, rounded to 300 V.

This is applies to the model by defining the electric field strength, F required for ionization.

$$F = \frac{V}{d} \tag{4.4}$$

Using Equation (4.4), 300 V needs to be applied across the 0.3175 cm separation of the anode nozzle and cathode accelerator grid for ionization to occur; therefore, we can assume an electric field strength of 94.475 kV/m is required to ionize the Argon gas.

THIS PAGE INTENTIONALLY LEFT BLANK

# V. RESULTS

The computer model was able to successfully model the electric field and its interaction with particles as they flowed through the area. Although some results are not as expected, the process of finite element modelling shows a good promise for system analysis and design. The following results will compare a blank thruster (the one without CNT grown) and a CNT deposited thruster.

## A. ELECTRIC FIELDS

The electric fields are simulated between the anode and cathode with both models. Figures 15 and 16 show the magnitude of the electric field with red signifying areas where the field magnitude is greater than the ionization requirement, known as the ionization area (IA), of Paschen's Law $E_{Field} > 94.475$ kV/m, when 250 volts is applied to the anode thruster nozzle and ground at the accelerator mesh grid. Blue areas are those where this requirement has not been met.

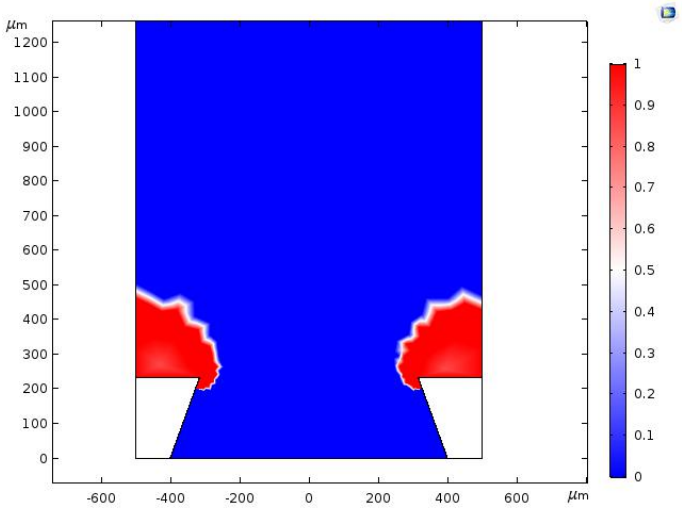


Figure 15. Electric field of blank sample at 250V

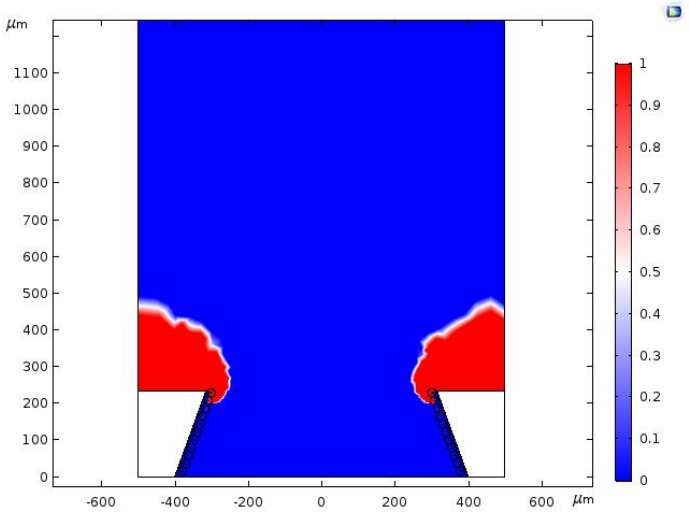


Figure 16. Electric field of CNT growth sample at 250V

The geometric electric field enhancement of the CNT when 250 volts is applied, is better shown in Figure 17, magnified into the edge of the mouth of each model's nozzle. It is clear in Figure 17B that localized IAs form at the tips of the CNTs. These IAs will facilitate ionization events to occur earlier in the particle path through nozzle.

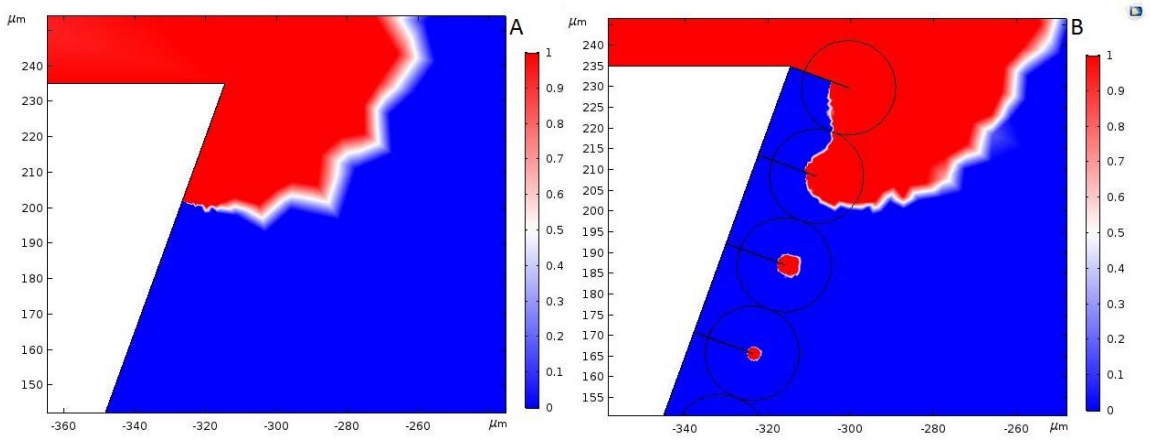


Figure 17. Zoomed electric field of both models at 250V

As the voltage applied to the anode is increased, the area that meets the ionization requirement increases around each CNT and eventually merges into a single, large IA, as shown in Figures 18 and 19.

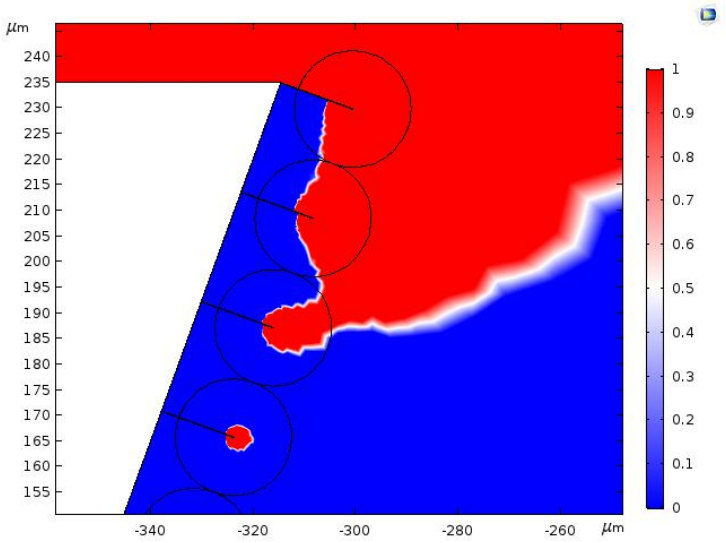


Figure 18. Zoomed electric field of CNT growth sample at 300V

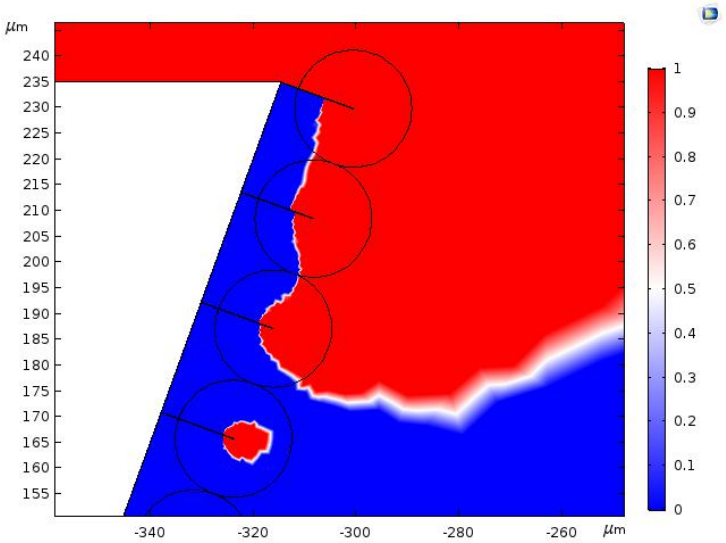


Figure 19. Zoomed electric field of CNT growth sample at 350V

This pattern of the increasing IA around the CNTs and merging together continues along the entire length of the nozzle wall and as the applied voltage is increased. As the released particles pass through the IA, they become ionized and begin to accelerate from the electric field effects on a charged particle.

## B. PARTICLE IONIZATION

One thousand particles were released at the bottom of the model with an initial vertical velocity of 1,523 m/s. The lower value of particles is used from the estimated two thousand before to reduce computation time per simulation while still providing viable data. As the particles pass through the electric field modelled, their charge value shifts from 0 to $1.9 \times 10^{-19}$ Coulomb when they pass through an ionization area. The charge of the particles will interact with the electric field and the x and y components of their velocities will increase as a function of the electrostatic force, shown in equation:

$$v = v_0 + E_{Field} \frac{e}{m} t \tag{5.1}$$

where $v_o$ is the initial velocity of the particle, $E_{Field}$ is the magnitude of the electric field at particle location, $e$ is the fundamental charge, $m$ is the mass of a single atom of argon and $t$ is the total time at a given time step. Figure 20 shows the trajectories of the particles. This is a comparison of a blank thruster and a CNT-covered thruster side by side.

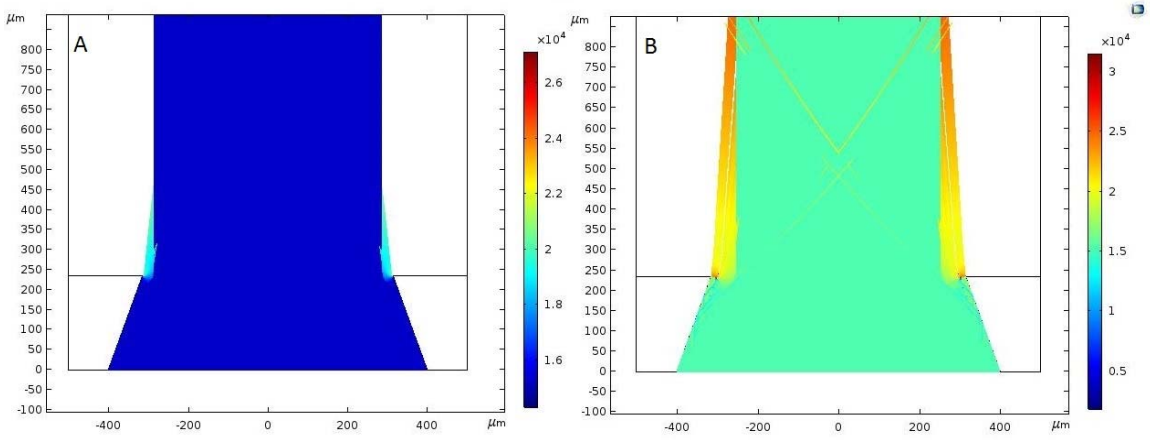


Figure 20. Ionization comparison (a) blank and (b) CNT growth models at 250 V

From the color legend to the right, signifying the particle velocities, it is clear that higher velocities are present in Figure 20B, the CNT growth model because the scale of velocity is larger than in Figure 20A, the blank model. Higher velocities are achieved

because some particles ionize earlier as they pass the IA near the tips of the CNTs, shown in Figure 21.

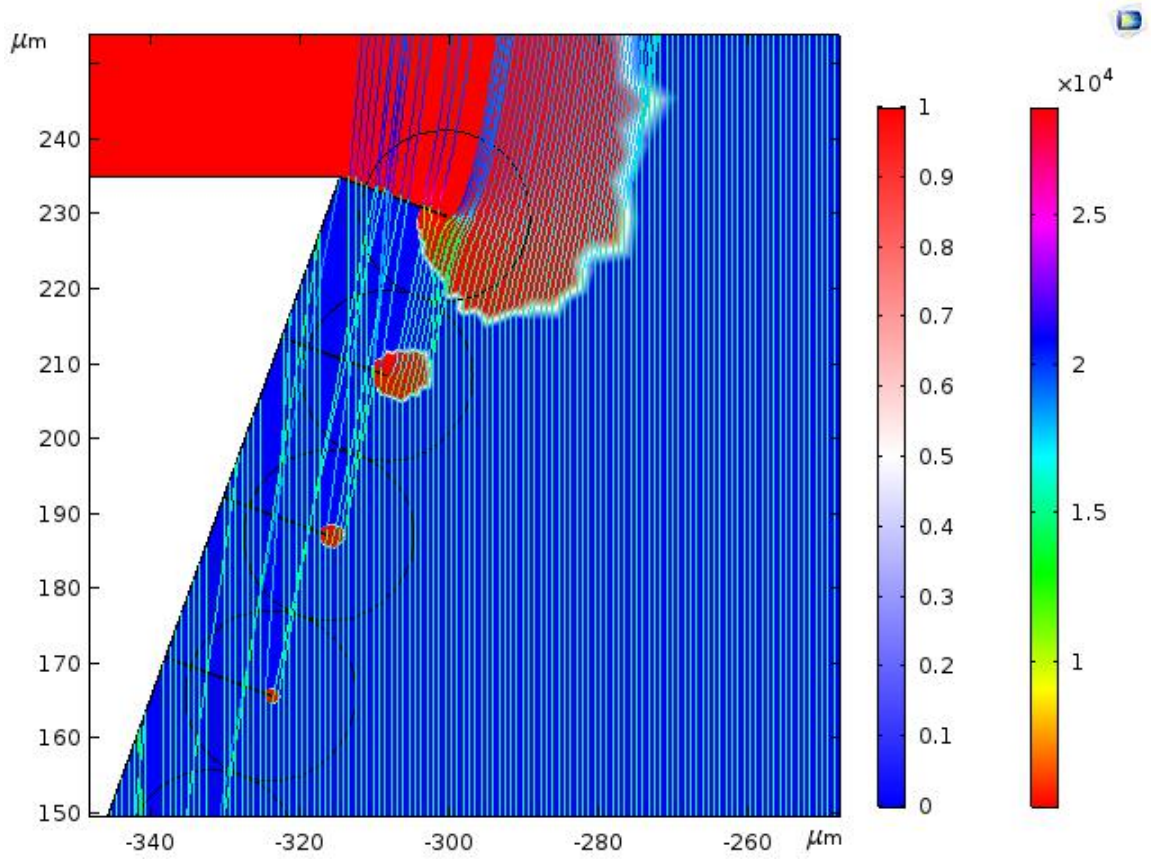


Figure 21. Particle ionization at CNT tip IA at 200 V applied

The sum of the velocities of all particles with ionization condition value of one was exported from the model and used to determine the total current provided by each model using equation 2.4. The current generated by the charged particles is plotted versus each applied voltage potential from 200 to 600 volts in Figure 22. This is for a blank sample that ionizes its particles at the Paschen ionization requirement of $E_{Field} \geq 94.475$ kV/m.

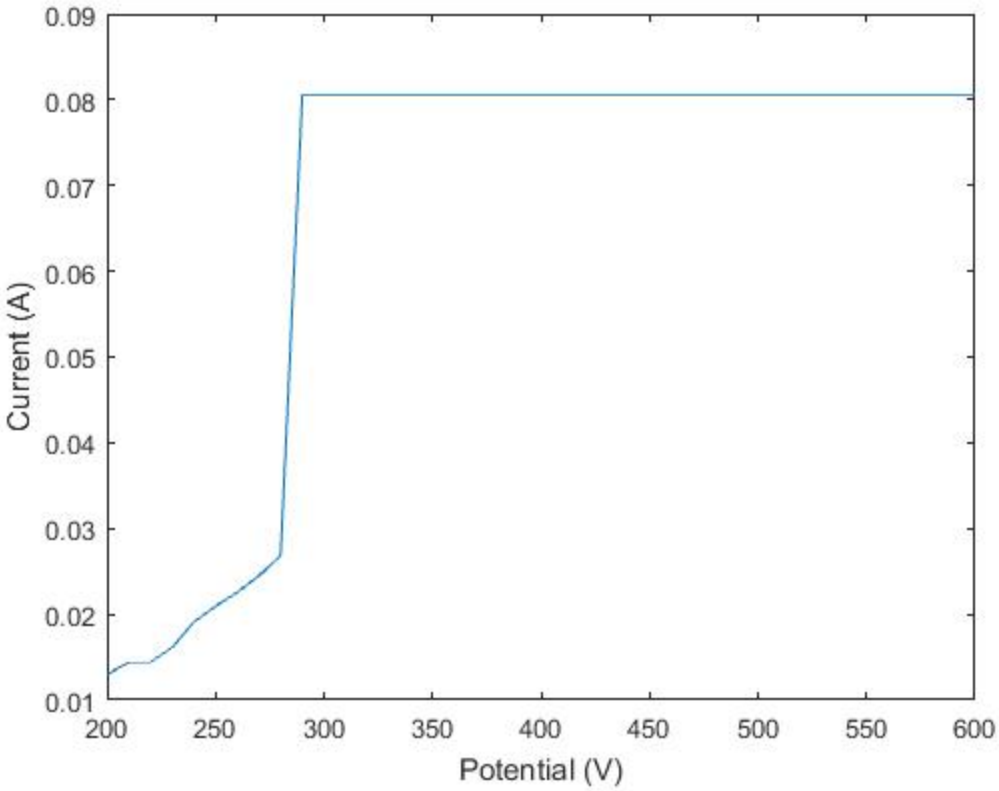


Figure 22. Ion current vs. voltage in blank sample at Paschen ionization

The ion current grows linearly up until 300V and then jumps to a plateau value and remains at that value for the remainder of the iterations. This is due to the IA encompassing the entire area and the model determines all particles ionizing, shown in Figure 23.

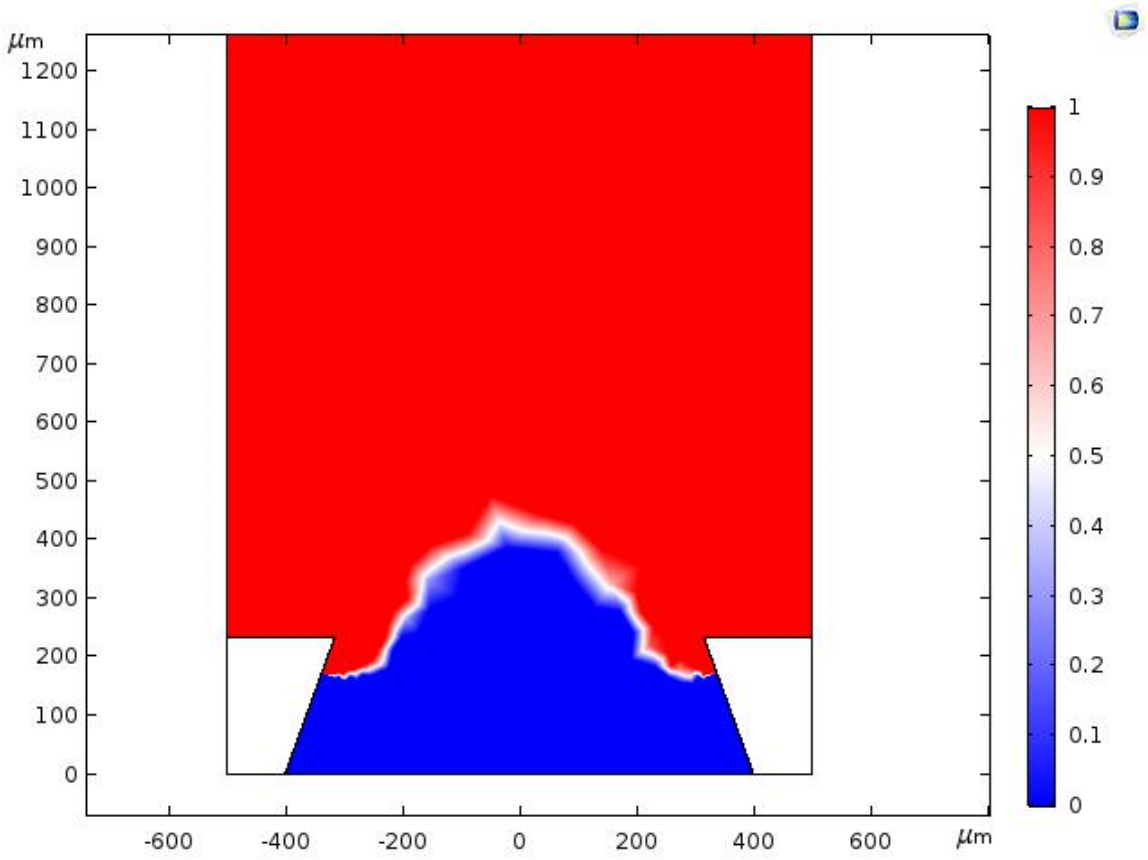


Figure 23. Ionization requirement encompassing entire area

The CNT sample shows the same trend, however the current generated between 200 and approximately 300 volts are larger, meaning more particles ionized in the CNT model than in the blank model. This is shown in Figure 24, with the blank sample currents and CNT sample currents overlaid.

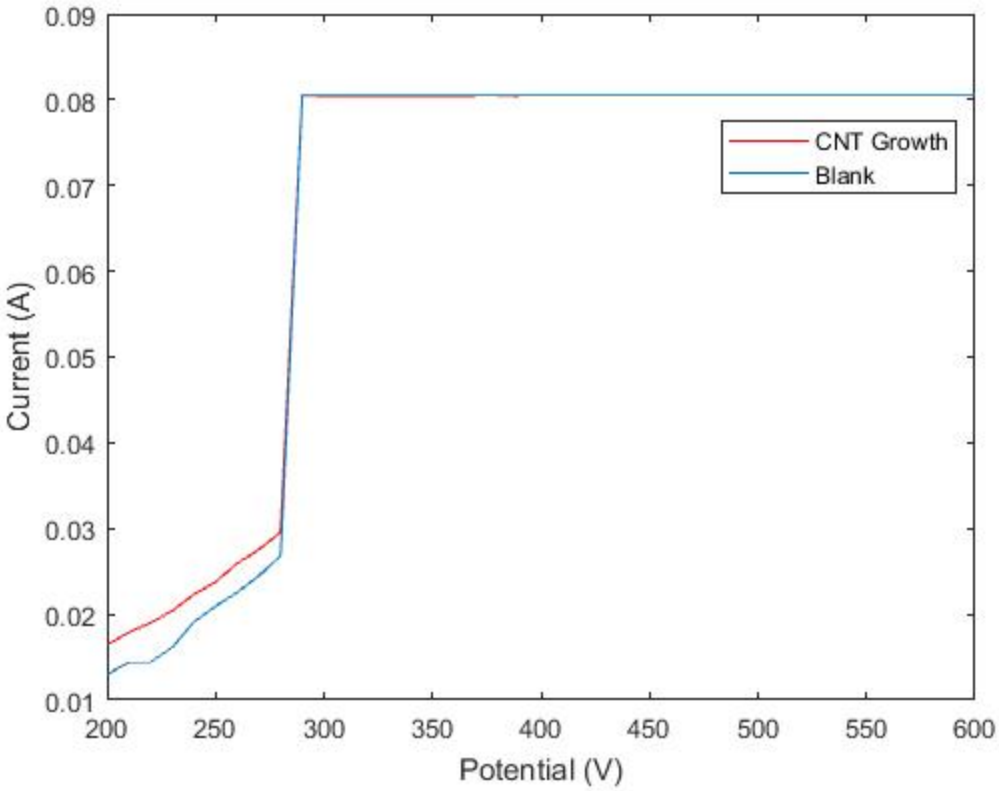


Figure 24. Ion current comparing blank to CNT sample

This relative comparison of nozzles with and without nanotubes is in good agreement with the same comparison of experimental data, collected by LT Bryan Crosby [12]. Figure 25 shows the currents collected from experimental samples, a blank and a CNT growth.

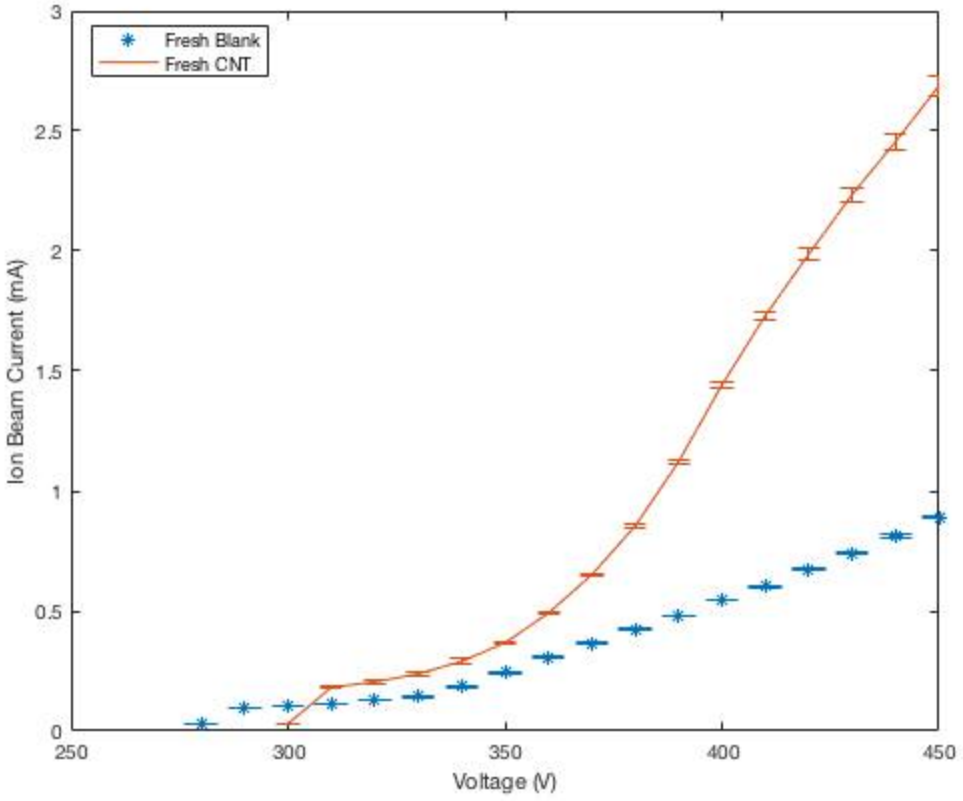


Figure 25. Comparison of experimentally collected currents between a blank sample and CNT growth sample at 3 g/h. Source: [12]

The experimental data is able to achieve a higher potential, however the trend and slope of the current to voltage relationship at initial currents observed agree with the simulation.

The use of Paschen's law for the requirement of ionization proved to be accurate to a point. When the IA was large enough to ionize all particles the MUF became one showing that this ionization requirement is no longer valid. This can be the case due to several causes. The ionization requirement initially used was developed for much simpler geometries and nozzle and nanotube geometries may be adding a layer of complexity. Another potential reason for this discrepancy may be because our simulation is not considering turbulence and fluid flow effects. Similar rapid increase in current is also observed experimentally after 350V (Figure 25), however it is believed this is due to a

cascading ionization event called the Townsend discharge [12], not investigated in this thesis. Between the experimental data and simulation results it is possible to determine the ionization parameters to further refine the accuracy of the simulation. By adjusting the ionization requirement to a higher value of $E_{Field} > 132$ kV/m we can allow comparison of relative current intensities with the experimental results. Figure 26 is the comparison and validation the accuracy of the model in the lower voltage regime.

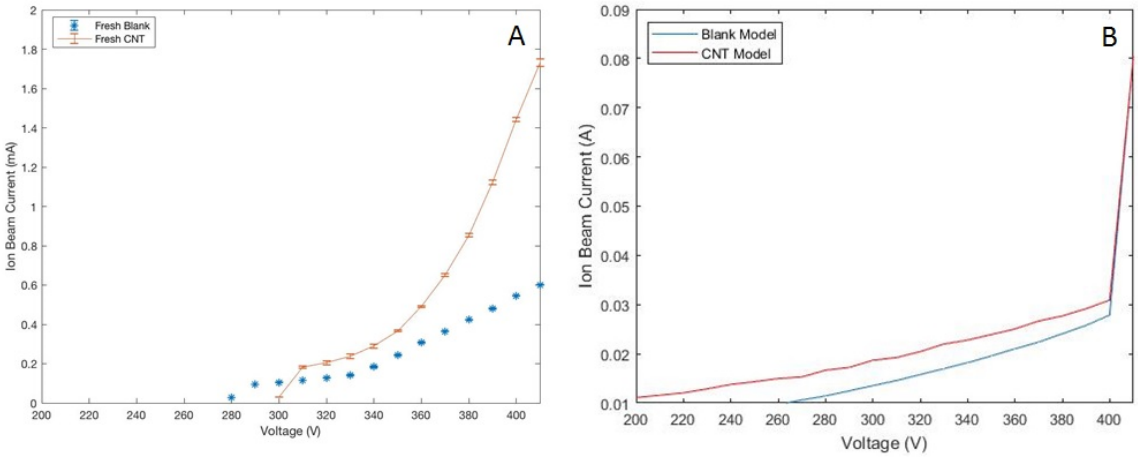


Figure 26. Experimental results (a). Source: [12];
model adjusted ionization requirement (b).

The scales of axes in Figure 26 have been adjusted to better see the trend comparison of the current to voltage relationship of both the simulation and experimental results.

# VI. CONCLUSION AND RECOMMENDATIONS

The trends and comparisons of two configurations in FEA simulation agrees with experimental data. Even with some basic assumptions for the ionization criteria, from assuming the assembly is like parallel plate geometry to using Paschen's law from previous experimental setups, there is still a notable improvement in ion beam current in a CNT growth model compared to a blank model. The electric fields generated by the CNT deposited model, generated IA electric fields earlier in the nozzle, resulting in ionizing the gas sooner than in the blank model, which ultimately results in a higher ion beam current.

## A. THRUSTER OPTIMIZATION

An accurate ionization model can allow for simpler and faster improvements to the thruster design. As the model ionization requirement is refined, different geometric shapes, CNT densities or event full 3D models can be rendered to test new ideas. This process can assist development by minimizing the timely and expensive iterative process of manufacturing MEMS devices while optimizing thruster design.

## B. RECOMMENDATIONS

The model is shows accurate comparison of the two designs only up to the moment when all particles are considered ionized. This is not what is happening experimentally. Different computer modelling modules need to be investigated to include other physical factors, such as fluid dynamics effects on the inlet gas as well as plasma physics effects between the nozzle and the accelerator grid. There is also the possibility of second stage ionization occurring, which cannot be modelled with current modules. The computer model has proven to be useful as a proof of concept and should be continued to be refined. When the simulation can accurately model the experimental results it will become a useful tool in improving the overall design of CNT enhanced micro ion thrusters.

THIS PAGE INTENTIONALLY LEFT BLANK

# APPENDIX. MATLAB DATA ANALYSIS CODE

```
clc
clear all

t = 3.3e-11;          %Time Step
to = 6.6e-8;          %Total Time
e = 1.6022E-19;       %Charge of an electron (C)
mdot = 3/(3600);      %g/s
M = 39.95;            %g/mole
a = 6.02214E23;       %Avogadro's number
ndot = a*mdot/(25*M); %particles per second per nozzle
nplane = ndot*t;      %particles in a plane per experiment

Data = csvread('Comsol_export',8, 0); %Particle velocities
Data(Data<=15230)=0;

for x=1:2:81
Ip = (2*e*Data(:,2+x))./((Data(:,1+x)+Data(:,2+x))*t);%Current of each
particle
Ip(isnan(Ip))=0;
i = sum(Ip);                                    %Total current of
plane
I(x) = (i/1000)*nplane;                         %Expected current of
plane
end

I(I==0)=[];

V=200:10:600;

plot (V, I);
xlabel('Voltage (V)');
ylabel('Ion Beam Current (A)');
hold all
```

THIS PAGE INTENTIONALLY LEFT BLANK

# LIST OF REFERENCES


[1] V. Kaushish, "Force limited vibration testing and subsequent redesign of the Naval Postgraduate School Cubesat launcher," M.S. thesis, Dept. of Astro. Eng., Naval Postgraduate School, Monterey, CA, USA, 2014. Available: https://calhoun.nps.edu/handle/10945/42656

[2] D. M. Goebel, and I. Katz. (2008). *Fundamentals of Electric Propulsion: Ion and Hall Thrusters*. Hoboken, NJ, USA: John Wiley and Sons, 2008.

[3] E. Y. Choueiri, "A critical history of electric propulsion: The first 50 years (1906-1956)," *J. of Prop. and Power*, vol. 20, no. 2, pp. 193–203, Mar.–Apr. 2004.

[4] H. D. Beckey, *Principles of Field Ionization and Field Desorption Mass Spectrometry*, Elsmford, NY, USA: Pergamon Press Inc., 1977.

[5] C. Torres, P. G. Reyes, F. Castillo, H. Martinez "Paschen law for argon glow discharge." *J. Phys.: Conf.,* Ser. 370 012067. [Online]. doi: 10.1088/1742-6596/370/1/012067

[6] R. Gomer, "Field emission, field ionization, and field desportation" *Surf. Sci.,*vol. 299/300, pp. 129–152, Jan 1 1994. [Online]. doi:10.1016/0039-6028(94)90651-3

[7] R. H. Fowler and L. Nordheim, "Electron emission in intense electric fields," *Proc. of the Royal Soc. A: Math, Phy. and Eng. Sci.*, vol. 119, pp.173–181, 1928.

[8] J. J. Hallan, "Carbon nanotube-based field ionization chamber for spacecraft propulsion applications," M.S. thesis, Dept. of Phy., Naval Postgraduate School, Monterey, CA, USA, 2012.

[9] A. P. Garvey, "Enhanced ionization of propellant through carbon nanotube growth on angle walls," M.S. thesis, Dept. of Phy., Naval Postgraduate School, Monterey, CA, USA 2017. Available: https://calhoun.nps.edu/handle/10945/55599

[10] A. D. Wold, "Carbon nanotube electrode development for ion thruster miniaturization," M.S. thesis, Dept. of Phy., Naval Postgraduate School, Monterey, CA, USA 2011.

[11] "200 Mesh copper data sheet, Part number 200X200C0020W48T, TWP INC.," Accessed November 20 2017. [Online]. Available: https://www.twpinc.com/tcpdf/pdf/create.php?prod_id=3960

[12] B. D. Crosby, “Field ionization test chamber for carbon nanotube-based miniature ion thruster applications,” M.S. thesis, Dept. of Phy., Naval Postgraduate School, Monterey CA, USA, 2017.

# INITIAL DISTRIBUTION LIST

1. Defense Technical Information Center
   Ft. Belvoir, Virginia

2. Dudley Knox Library
   Naval Postgraduate School
   Monterey, California